

Site of pegylation and PEG molecule size attenuate interferon-alpha anti-viral and anti-proliferative activities through the JAK/STAT signaling pathway.

Michael J. Grace¹, Seju Lee², Sheri Bradshaw¹, Jeffrey Chapman¹, Jeffrey Spond¹,
Stuart Cox¹, Marc DeLorenzo¹, Diana Brassard³, David Wylie², Susan Cannon-Carlson²,
Constance Cullen¹, Stephen Indelicato¹, Marcio Voloch², and Ronald Bordens¹.

*Schering-Plough Research Institute, Biotechnology Development, Bioanalytical¹ and
Process Development², 1011 Morris Ave., Union, NJ 07083. Aventis Pharmaceuticals,
Medical Affairs-Oncology³, Bridgewater, NJ 08807.*

Corresponding Author:

Michael J. Grace, Ph.D.

1011 Morris Ave.

Union, NJ 07083

Ph (908) 820-6816

Fax (908) 820-6720

michael.grace@spcorp.com

Running title: Influence of pegylation on interferon efficacy

Abstract

Therapeutic pegylated interferon alphas (IFN- α) are mixtures of positional isomers that have been mono-pegylated at specific sites on the core IFN- α molecule. The pegylation results in lower *in vitro* specific activity associated with the core IFN- α molecule that is related to the site of pegylation and size of PEG attached. We prepared purified, homogeneous, positional pegylation isomers of IFN- α 2b that were mono-pegylated using 5 kD to 30 kD linear PEG molecules attached at 7 primary reactive amino acid residues: Cys¹, His³⁴, Lys³¹, Lys⁸³, Lys¹²¹, Lys¹³¹, and Lys¹³⁴. The isomers were evaluated for STAT translocation and anti-viral and anti-proliferative activity. The site of pegylation strongly influenced activity relative to an IFN- α 2b control. The highest residual activity was observed with the His³⁴ positional isomers and the lowest with the Cys¹ positional isomers. The Lys positional isomers demonstrated intermediate activity, with a general order of Lys¹³⁴ > Lys⁸³ ~ Lys¹³¹ ~ Lys¹²¹ > Lys³¹. The progressive relationship between decreased activity and increased PEG size suggests that pegylation may interfere with interaction and binding of IFN- α to the IFNAR1/IFNAR2 heterodimeric receptor. The higher specific activity associated with the His³⁴ positional isomer suggests that this site may be favorable for pegylating IFN- α 2b molecules.

Introduction

Chronic hepatitis C is considered one of the major causes of chronic liver disease, cirrhosis and hepatocellular carcinoma, and is the most common reason for liver transplantation in the US(1). It is estimated that there are 3 million chronically infected individuals in the US, and over 170 million worldwide (1). Treatment of hepatitis C has evolved from the use of interferon-alpha (IFN- α) either alone or in combination with ribavirin, to the newer pegylated interferons (PEG-IFNs), which have provided a dramatic increase in virological response, especially in combination with ribavirin. Standard IFN- α therapy has a short (<12 hour) half-life that requires thrice-weekly subcutaneous injection to maintain effective levels in the blood (2). The short half-life of IFN- α has led to the development of longer-lasting preparations achieved by the attachment of a large polyethylene glycol (PEG) molecule directly to IFN- α . Two different commercial preparations of PEG-IFN- α have been developed for clinical use, PEG-IFN- α 2b (PEG-INTRON[®]) and PEG-IFN- α 2a (Pegasys[®]); both have long half-lives (40 and 80 hours, respectively) that permit once-weekly administration (3). Both of these preparations have been demonstrated to be effective for the treatment of patients with hepatitis C (4), and clinical trial results have shown further that both of the pegylated molecules produce sustained viral response (SVR) rates superior to those achieved with their respective standard IFN- α s (5-7).

While pegylation has proven to be highly effective for slowing the clearance of biological molecules, including IFN- α , and thus increasing serum half-life, it has been shown to also modify *in vitro* biological activity (8). For instance, we have reported that pegylation

of IFN- α 2b with 12-kD linear PEG molecule results in a preparation that is 28% relative in specific activity compared with IFN- α 2b; the loss in activity was not due to structural perturbation of the core IFN- α 2b core protein (9). Other groups have reported that pegylation of IFN- α 2a with 40 kD branched PEG molecule results in a preparation that contains from 1% to 7% relative specific activity compared with IFN- α 2a (10,11). These two pegylated interferon- α s (PEG-IFN- α s) differ substantially in their post-pegylation constituent properties. PEG-IFN- α 2b has a 12 kD linear PEG molecule attached using SC-PEG chemistry via a covalent urethane-like bond to the IFN- α 2b protein (12). The pegylation linkage process results in a heterogeneous mixture of pegylation positional isomers that occur predominantly (~50%) at the His³⁴ amino acid residue with the remaining positional isomers pegylated at various lysines, the N-terminal cysteine, a serine, tyrosine, and an alternate histidine residue (12). PEG-IFN- α 2a has a 40-kD branched PEG molecule attached using NHS-PEG chemistry via a covalent amide bond to the IFN- α 2a protein (11). PEG-IFN- α 2a is also a heterogeneous mixture of pegylated positional isomers consisting of 4 major positional isomers at Lys³¹, Lys¹²¹, Lys¹³¹, and Lys¹³⁴ (10).

The different relative specific activities reported for the IFN- α preparations suggested that the significant differences in the size of the PEG molecule or the distribution of pegylation positional isomers, or both, might be accountable. Fractionation of specific pegylation positional isomers for 12 kD PEG-IFN- α 2b have demonstrated that positional isomers had differential relative specific activities, with the His³⁴ positional isomer retaining higher relative activity (37%) than the mixture of positional isomers (9). Thus,

changes in the activity of pegylated proteins appear to be influenced by the site of pegylation and, in some cases, the molecular weight of the PEG moiety (13).

Our study was undertaken to directly determine the effects of size and site of pegylation on *in vitro* activity for IFN- α 2b. This information is important for understanding how specific characteristics of PEG-IFN- α s influence their *in vitro* activity that may be translated to their *in vivo* efficacy.

Materials and Methods

IFN- α 2b (Intron[®] A) and 12 kD PEG-IFN- α 2b (PEG-INTRON) were manufactured by Schering-Plough Corp (Kenilworth, NJ). The IFN- α 2b international reference standard (95/566) was kindly provided by the National Institute for Biological Standards and Control (NIBSC, South Mimms, Hertfordshire, UK) (14). The specific activity for IFN- α 2b, used as starting material in these studies, was 2.6×10^8 IU/mg, as calibrated against 95/566. IFN- α 2a (Roferon[®]-A) and 40 kD PEG-IFN- α 2a (Pegasys) were manufactured by Hoffmann-La Roche Inc (Nutley, NJ). IFN- α 2a was purchased and used directly from the commercial stock solution of 36 MIU/mL, which has a protein concentration of 133.3 μ g/mL. For this study, the specific activity of IFN- α 2a was determined empirically to be 2.4×10^8 IU/mg when calibrated against the IFN- α 2b reference standard in the anti-viral assay. The 40 kD PEG-IFN- α 2a was purchased and used directly from the commercial stock solutions of 135 μ g/mL and 180 μ g/mL. Protein concentrations for IFN- α 2a and 40 kD PEG-IFN- α 2a were confirmed prior to use. Succinimidyl carbonate polyethylene glycol (SC-PEG) linkers with average PEG molecular weights of 5, 12, 20, and 30 kD were purchased from Shearwater Polymers (Nektar Therapeutics, San Carlos, CA).

Production and isolation of pegylated interferon isomers for activity studies. The primary reactive amino acid residues of IFN- α to pegylation are Cys¹, Lys³¹, His³⁴, Lys⁸³, Lys¹²¹, Lys¹³¹, and Lys¹³⁴. His³⁴ and Cys¹ are most reactive at a neutral pH, whereas the ϵ -amine groups of lysine residues are most reactive at basic pH (15). Therefore, pegylation reactions utilizing SC-PEG 5 kD, SC-PEG 12 kD, SC-PEG 20 kD, and SC-PEG 30 kD

were performed at room temperature at pH 6.5 to produce His³⁴ and Cys¹ modified positional isomers and pH 10 to produce the ϵ -amine modified lysine positional isomers.

Reactions at pH 6.5 were performed in 50 mM sodium phosphate at 22°C, with SC-PEG 5 kD, SC-PEG 12 kD and SC-PEG 20 kD present in 4.2-fold molar excess relative to IFN- α 2b (5 mg/mL). For the reactions involving SC-PEG 30 kD, the linker-to-protein molar ratio was limited by linker solubility to 2:1. After 70 minutes, reactions were quenched with 1M glycine to minimize the formation of multi-pegylated species.

Reactions at pH 10 were performed in 30 mM sodium tetraborate at 22°C. Due to the increased rate of reaction at this pH, the molar ratio of linker to protein was reduced to 1.0 for SC-PEG 5 kD, SC-PEG 12 kD, and SC-PEG 20 kD. To adjust for the reduced reactivity of higher molecular weight (MW) PEG polymers, the ratio was increased to 1.5 for SC-PEG 30 kD. Reactions were again quenched with 1 M glycine.

Quenched reaction products were dialyzed against 100 mM sodium phosphate, 150 mM NaCl pH 5.0 at 5°C. Mono-PEG-IFN- α 2b was purified from dialysates by size exclusion chromatography on a Superdex 200 HiLoad column (26 mm \times 60 cm, 34 \pm 10 μ m particle size; Amersham). All pools contained at least 98% mono-PEG-IFN- α 2b as assessed by high-performance size-exclusion chromatography (HPSEC, Superdex 200 HR, 10 mm \times 30 cm, 13 μ m particle size; Amersham). The primary contaminant was di-PEG-IFN- α .

Single PEG-IFN- α 2b positional isomers were isolated from the mono-PEG- IFN- α 2b pools by high-performance ion exchange chromatography (HPIEX) on a preparative scale sulfopropyl (SP) column (21.5 mm \times 15.0 cm, 13 μ m particle size; TosoHaas, Philadelphia, PA) using a Waters HPLC system (717+ Autosampler with a 2.5 mL syringe, 486 Detector, 2 510 HPLC pumps with high-pressure gradient mixing, 6 ml/min flowrate) with monitoring by ultraviolet (UV) light at 280 nm. This procedure, previously utilized to resolve positional isomers of 12 kD PEG-IFN- α 2b (15), was optimized to improve the resolution of positional isomers with varying PEG molecular weights. The purified mono-PEG-IFN- α 2b size exclusion pools were dialyzed overnight at 5°C against HPIEX buffer A (1.8 mM citric acid monohydrate, 3.3 mM sodium phosphate dibasic heptahydrate, pH 5.3). The dialysates were concentrated to 2.2 A₂₈₀ prior to loading onto the SP column, pre-equilibrated with buffer A. Loading was adjusted over a range of 19–65 μ g protein/mL of resin. Bound positional isomers were eluted using pH gradients formed by buffer B (30 mM trisodium citrate dihydrate, 70 mM sodium phosphate monobasic monohydrate, pH 6.0). To optimize resolution of positional isomers, the pH gradient was adjusted according to both attached PEG length and site of pegylation. As can be seen in Figure 1a, the His³⁴ and Cys¹ positional isomers are well resolved from other positional isomers generated at a reaction pH of 6.5 when eluted with a gradient of 0-10% B in 100 min, followed by 10-30% B over 80 min. The separation of lysine-modified 12 kD PEG-IFN- α 2b positional isomers also involved 2 sequential linear gradients; from 0%–14% buffer B in 180 minutes followed by 14%–20% buffer B in 40 minutes. Due to weaker binding to the SP column, shallower gradients (0%–12% buffer B in 180 minutes followed by 12%–15% buffer B in 40 minutes) were employed to elute

higher MW PEG-IFN- α 2b lysine-modified positional isomers (Figure 1b). Peak fractions were manually collected in order to generate pools consisting of of single positional isomers. The purity and identity of the positional isomers were assessed by HPSEC, analytical HPIEX (SP-5PW, 7.5 mm \times 7.5 cm, 10 μ m particle size; TosoHaas) and peptide mapping followed by amino acid sequencing. There was no detectable free IFN- α in any of the purified positional isomer pools by HPSEC.

Stability of positional isomer pools. Evaluation of the pools by HPSEC following five freeze/thaw cycles to simulate handling conditions demonstrated that the positional isomers were stable and the pools remained free of IFN- α contamination.

Peptide mapping. Characterization of purified positional isomer peaks was carried out as previously described (15). Peak fractions were concentrated to 0.5–1 mg/mL using a centrifugal spin filter (Ultrafree 15 mL, BioMaxx 50; Millipore). After adding a 10% (v/v) aliquot of 50 mM ammonium bicarbonate, the concentrate was digested with trypsin (1:10 m/m) overnight at 37°C. Dithiothreitol (DTT, 100 mM) was added to a final concentration of 5 mM, and incubation was carried out for 1 hour at ambient temperature. The reduced digest was resolved by HPSEC with manual collection of pegylated peptides. The entire pegylated peptide peak was pooled and characterized by N-terminal sequence analysis. All peptide sequencing was performed by Commonwealth Biotechnologies (Richmond, Virginia) using Agilent hardware.

Production and isolation of branched 20 kD PEG-IFN- α 2b and di 20 kD PEG-IFN- α 2b for estimation of Stoke's Radius. Two additional preparations of pegylated IFN- α 2b were made solely for the study of the effect of pegylation on Stoke's radius. Branched 20 kD PEG-IFN- α 2b was produced by using PEG2-NHS 20kD at a 2:1 molar ratio. Pegylation was performed at pH 8.8 at 22°C in 40 mM sodium tetraborate with quenching at 60 minutes using 1M glycine. The reaction mixture was isolated and purified as described for the positional isomers used for activity measurements.

Di 20 kD PEG-IFN- α 2b was produced as a secondary product from the SC-PEG reactions at pH 10. The mixture was purified from pegylation reaction by collecting the unbound fraction obtained from anion exchange chromatography on Q HyperD (BioSeptra). The reaction products were dialyzed against 10 mM sodium phosphate, pH 8.2. The dialyzed product was applied at 1.4 mg protein per mL resin to a 20 cm column with a flow of 1.66 cm/min. Di-pegylated IFN- α was collected from the unbound fraction. This fraction was further purified by size exclusion chromatography on Superdex 200 HiLoad under conditions identical to those used for the purification of monopegylated interferon alpha. The purity of di-pegylated IFN- α purified by these columns was > 99% by SE-HPLC.

STAT1 translocation assay. Human hepatoma (Huh-7) cells were cultured in Dulbecco's Modified Eagle's Medium (DMEM), 10% fetal bovine serum, 2 mM GlutaMax-1, 100 U/mL penicillin-streptomycin, and nonessential amino acids. Cells (10,000 cells/well) were seeded overnight in 96-well Packard black view plates (Packard Instruments,

Meriden, CT). Three-fold serial dilutions of the test IFN- α s were prepared in DMEM and incubated with cells at 37°C in 5%–6% CO₂ for 30 minutes. The cells were washed with phosphate-buffered saline (PBS), fixed with 3.7% formaldehyde, and permeabilized with 0.5% Triton X-100. The cells were then incubated with either a polyclonal anti-STAT1 p84/p91 (clone E-23, Santa Cruz Biotechnology, Santa Cruz, CA) or a polyclonal anti-STAT2 (clone C-20, Santa Cruz Biotechnology, Santa Cruz, CA) primary antibody for 1 hour at room temperature. The cells were sequentially washed with PBS and 0.01% Tween-20. They were then incubated for 1 hour with a mixture of Alexa Fluor[®] 488 conjugated goat anti-rabbit IgG (Molecular Probes, Eugene, OR) and Hoechst 33342 (Molecular Probes). The cells were again washed with 0.01% Tween-20 and PBS. The plates were imaged on the ArrayScan[®] II High Content Screening System (Cellomics, Pittsburgh, PA) with a 10x objective using the ArrayScan v2.1 software (Cellomics). The resulting images were processed using the Cytoplasm to Nucleus Translocation Application Software (Cellomics). The cyto-nuclear difference, defined as the difference in fluorescence intensity of the target STAT in the nuclear region minus the cytoplasmic region, was used as a measure of STAT translocation. Cytoplasmic and nuclear STAT1 levels were also examined for each cyto-nuclear difference determination. We confirmed that the cyto-nuclear difference was primarily caused by an increase in nuclear STAT1, while cytoplasmic STAT1 levels remained constant or only decreased slightly. This observation was consistent with data reported for TNF- α mediated NF- κ B cyto-nuclear translocation measurement using this instrumentation and software (16).

Anti-viral and anti-proliferation assays. The anti-viral assay was performed by titrating serial 2-fold dilutions in 96-well microtiter assay plates seeded with either human foreskin fibroblast cells (FS-71), or non-small cell lung carcinoma cells (A549) infected with encephalomyocarditis virus (EMCV) as previously described (17). The relative potency of IFN- α 2b and all the PEG-IFN- α s tested was determined by comparing the dose of the test preparation, which affords 50% protection to infected cells, with the dose of control IFN- α 2b reference standard. The IFN- α 2b standard was calibrated against the NIBSC IFN- α 2b (95/566) standard. The materials for the PEG-IFN- α s were dose-ranged in preliminary experiments to assure that potency would be determined across a suitable response range. Specific activities for 12 kD PEG-IFN- α 2b and 40 kD PEG-IFN- α 2a were calculated from the empirically determined titer at 50% protection divided by the calculated IFN- α 2b protein weight at the 50% point.

The anti-proliferation assay was performed by titrating serial 2-fold dilutions in 96-well microtiter assay plates seeded with Daudi cells. Daudi cells (ATCC), a human lymphoblastoid cell line, were cultured in Dulbecco's modified Eagle's medium supplemented with 10% fetal bovine serum. After a 72-hour incubation, cells were treated with 3-(4,5-dimethylthiazol-2-yl)-2,5-diphenyltetrazolium bromide (MTT)/sodium dodecyl sulfate (SDS) and analyzed spectrophotometrically for cellular mitochondrial activity associated with viability. The relative potencies of IFN- α 2b and all the PEG-IFN- α s tested were determined by comparing the dose of the test preparation, which induced a 50% decrease in formazon-determined proliferation, with the dose of control IFN- α 2b reference standard. The IFN- α 2b standard was calibrated

against the NIBSC IFN- α 2b (95/566) standard. For the PEG-IFN α s, materials were dose-ranged in preliminary experiments to assure that potency would be determined across a suitable response range. Specific activities for 12 kD PEG-IFN- α 2b and 40 kD PEG-IFN- α 2a were calculated from the empirically determined titer at 50% proliferation divided by the calculated IFN- α 2b protein weight at the 50% point.

Statistical analysis of STAT translocation and anti-viral data. The 50% inflection point for each of the dose-response curves of the STAT translocation responses and the anti-viral responses were determined using iterative curve fitting software. SoftMaxPro version 4.3 (Molecular Devices) software was used for reducing the STAT translocation data. A proprietary version of AllFit, Allwin 2.03, was used for reducing the anti-viral data. The descriptive statistics were generated using SAS JMP version 5.0.1 (SAS). An analysis of variance was carried out using Student's, Tukey-Kramer, Dunnett's, and Hsu MCB. All comparisons were first carried out against the respective PEG size isomer of His³⁴. Additional comparisons were also conducted looking at the effect of PEG size change within each isomer. Other analyses for Lysine comparisons in the anti-viral assay were also performed. In selective cases where the variances were flagged as unequal, a Welch ANOVA test was also carried out to confirm results. Because the STAT translocation assay was more variable than the anti-viral assay, the Student's t-test was a more rugged comparator of variance.

Determination of Stokes Radius of PEG-IFN- α 2b. The apparent molecular weights and Stokes radii of 5 kD, 12 kD, and 20 kD PEG-IFN- α 2b, branched 20 kD IFN- α 2b

(containing a PEG moiety with 2×10 kD PEG branches for a total molecular weight of 20 kD) and a di-PEG 20 kD IFN- α 2b (containing 2 linear 20 kD PEG molecules attached to the protein at 2 different sites, for a total molecular weight of 40 kD) were determined. The 5 kD, 12 kD, 20 kD, branched 20 kD and di-PEG 20 kD IFN- α 2b were produced using SC-PEG chemistry and purified as preparations of mixed positional isomers. Apparent MWs were obtained from a standard curve (log MW versus retention time (RT) by HPSEC analysis) constructed using ten different marker proteins. The R_s for the PEG-IFN- α 2bs were then calculated based on a standard curve of log R_s versus log MW also obtained using these markers. HPSEC analysis of the PEG-IFN- α 2bs was performed using a Sigma ChromTM GFC-1300 column (12–15 μ m particle size; Sigma-Aldrich, Inc., St. Louis, MO) in 0.1 M sodium phosphate and 0.1 M NaCl, pH 7.0 at a flow rate of 0.5 mL/minute.

Results

Confirmation of differential activity between 12 kD-mono-pegylated IFN- α 2b and 40 kD-mono-pegylated IFN- α 2a. Because the reported activity for 12 kD-mono-pegylated IFN- α 2b and 40 kD-mono-pegylated IFN- α 2a was generated from different laboratories using different anti-viral assays, we first measured the differential activity directly. 12kD PEG-IFN- α 2b was consistently more than 25-fold more active than 40 kD PEG-IFN- α 2a in an anti-viral protection assay using either FS-71 or A549 cells (Table 1). The activity of 12 kD PEG-IFN- α 2b ranged between 25% and 35% of that for IFN- α 2b control, values comparable to those previously reported (9). The activity of 40 kD PEG-IFN- α 2a was approximately 1% of that for IFN- α 2b. This value is lower than that from one previous report (10), but consistent with those from another recent evaluation of the activity of PEG-IFN- α 2a in the Madin-Darby bovine kidney anti-viral assay (11). IFN- α 2a, the core interferon protein for 40 kD PEG-IFN- α 2a, was titrated in the FS-71 anti-viral assay with IFN- α 2b and was found to be equivalent in activity within variation of the assay. Thus, the lower activity seen with the 40 kD PEG-IFN- α 2a versus 12 kD PEG-IFN- α 2b cannot be accounted for by differences in the core proteins in the assay. In addition, circular dichroism spectroscopy revealed no perturbation in the near or far UV for the core protein of 40 kD PEG-IFN- α 2a (data not shown).

Results obtained in a Daudi cell anti-proliferation assay were similar to those for the anti-viral assay (Table 1). The specific activity of 12 kD PEG-IFN- α 2b was 28.9% of that for IFN- α 2b as compared to a value of 0.7% obtained for 40 kD PEG-IFN- α 2a.

Effect of PEG molecule size on PEG-IFN- α 2b Stokes radius and apparent molecular weight. Because of the hydrophilic nature of PEG polymers, increased polymer length can significantly increase the relative Stokes radius of a pegylated protein (18). In addition, due to the linear nature of the PEG moiety, the increase in the apparent molecular weight of a globular protein such as IFN- α 2b is much greater than the sum of the molecular weights of the protein and the attached PEG group. Using SC-PEG chemistry, we purified mixed positional isomer preparations of 5 kD, 12 kD, linear 20 kD, branched 20 kD, and di-20 kD PEG IFN- α 2b and measured the apparent molecular weight (aM_f) and Stokes radius (R_s) using HPSEC analysis. The addition of a 5 kD PEG group to IFN- α 2b increased the aM_f to 73.3 kD, a value of more than 3 times the additive molecular weight of the 23.1 kD protein and the 5 kD PEG group and the R_s was increased by 58% (Table 2). With the addition of the 12 kD PEG, the R_s increased by 119% relative to IFN- α 2b and the aM_f to 165.6 kD. The branched and linear 20 kD PEGs increased R_s by 166% and 184% relative to IFN- α 2b, and aM_f to 272.3 and 320.6 kD, respectively. For the di-20 kD PEG (with a total MW of 63.1 kD), the R_s was 275% higher than IFN- α 2b, and the aM_f was 639.7 kD. This increase in R_s as pegylated moieties increase in size or position might have implications for receptor binding, activation, and clinical efficacy.

Production and isolation of pegylated positional isomers of IFN- α 2b.

Pegylated positional isomers at Cys¹, His³⁴, Lys³¹, Lys⁸³, Lys¹²¹, Lys¹³¹, and Lys¹³⁴ were chosen for study because they have been reported as being major positional isomers for 12 kD PEG-IFN- α 2b or 40 kD PEG-IFN- α 2a (10,12). All reaction products were

resolved by size exclusion chromatography to generate mono-PEG-IFN- α that was >99% pure by HPSEC. These mono-pegylated reaction products were then resolved into individual positional isomers by HPIEX (Figures 1a & 1b) to 98% purity by HPSEC and 91%–99% purity by analytical HPIEX (15). Peptide mapping analysis can usually detect >5% impurities. However, one exception is the inability to resolve by HPIEX the neighboring peaks of 5 kD Lys¹³¹ and 5 kD Lys¹⁶⁴, hence, the lower purity estimation by analytical HPIEX relative to HPSEC. The HPIEX chromatography profiles and positional isomer elution order in this study matched those reported previously (12,15,19). In addition, the identity and purity of the purified positional isomers was confirmed by peptide mapping analysis.

STAT1 translocation studies. To study the effect of pegylation size and site on JAK/STAT IFN- α signal transduction, an assay was developed to assess STAT1 translocation from the cytoplasm to the nucleus in Huh-7 cells. The STAT1 translocation activity for the titration curves of each of the 7 positional isomers at each respective PEG molecule size is shown in Figure 2. The ED₅₀ (inflection points) for the positive control curves of 12 kD PEG-IFN- α 2b and 40 kD PEG-IFN- α 2a ranged from 2.0–4.8 and 33.0–76.0 ng/mL respectively across the experiments in Figure 2; a statistical analysis (USP 27 < 111>) determined that none of the control infection points were outliers. This variation is consistent with newly developed cell-based bioassays. Assay results showed that the 12 kD PEG-IFN- α 2b was more active than the 40 kD PEG-IFN- α 2a. The STAT1 translocation activity for the His³⁴ positional isomer was consistently similar to that for 12 kD PEG-IFN- α 2b. There was also little significant reduction in STAT1 translocation

activity for the His³⁴ positional isomers from 5 kD through 30 kD (Figure 2A). The Lys³¹ positional isomers exhibited less STAT1 translocation activity, demonstrated by a rightward shift in the titration curve, as the size of the PEG molecule increased from 5 to 30 kD (Figure 2B). The 5 kD Lys³¹ PEG-IFN- α 2b isomer had less translocation activity than 12 kD PEG-IFN- α 2b control curve (Figure 2B). Similar trends of decreased translocation activity associated with increasing PEG molecule size were observed with the other Lys and Cys positional isomers (Figure 2C-G).

The ED₅₀ was calculated for each of the site-pegylated IFN- α 2b isomers at PEG molecule sizes from 5 through 30 kD PEG (Figure 3). The His³⁴ positional isomers at 5 through 30 kD were the most active for STAT1 translocation, and increasing PEG molecule size at His³⁴ had only a small effect on STAT translocation activity. Cys¹ and Lys³¹ had the lowest translocation activity across all PEG molecule sizes, and both were very sensitive to increasing PEG molecule size above 5 kD. The STAT1 translocation activity for each different-sized PEG positional isomer for both Cys¹ and Lys³¹ were significantly different ($p < 0.05$, Student's t-test) compared with the respective His³⁴ positional isomer. The Lys¹³⁴ positional isomer trended to be the most active for STAT translocation of the lysine isomers studied, while the Lys⁸³, Lys¹²¹, and Lys¹³¹ isomers were roughly equivalent in their respective STAT translocation activities. These four lysine positional isomers also appeared to trend to lower STAT1 translocation activity compared with the His³⁴ positional isomer, although statistical significance was observed only with the 5 kD Lys⁸³ and 20 kD Lys¹²¹. For all of these positional isomers, there was

a consistent decrease in translocation activity associated with increased PEG molecule size to 20 or 30 kD.

Anti-viral protection activity of pegylated positional isomers. The same site and size pegylation isomers were also studied using an anti-viral protection assay in FS-71 cells. Overall, the results from the anti-viral assay (Figure 4) were consistent with the STAT1 translocation results. The most active positional isomer was His³⁴, and the least active were Cys¹ and Lys³¹. The most active lysine positional isomer was Lys¹³⁴, while Lys⁸³, Lys¹²¹, and Lys¹³¹ were roughly comparable in activity. Of note, all different-sized PEG positional isomers, compared against the respective His³⁴ positional isomer, were significantly lower ($p < 0.05$) in antiviral activity. However, the Lys¹³⁴ positional isomer, although lower in activity than His³⁴, was statistically the most active of the lysine positional isomers studied. In addition, significant decreases occurred ($p < 0.05$) in the anti-viral protection activity associated with increasing PEG molecule size for each of the positional isomers studied. These results confirm the significant differences and trends that were observed in the STAT1 translocation assay.

Discussion

Our initial studies were performed using unfractionated PEG-IFN- α 2a and PEG-IFN- α 2b, which are known to be mixtures of positional isomers (10,12). These results confirmed that there was a consistent 25–35-fold difference between the *in vitro* anti-viral and anti-proliferative activities of the two different PEG-IFN- α mixtures. The differences in relative activities between 12 kD PEG-IFN- α 2b and 40 kD PEG-IFN- α 2a may result from the different sizes of the PEG moieties, the different distribution of site-pegylated isomers, differences in the core IFN- α alpha proteins, and/or differences in the bonds linking the PEG molecules to their respective core protein (4,20). It is unlikely that differences between the activities of the core proteins, IFN- α 2a and IFN- α 2b, contribute to the observed differences between the two pegylated preparations since their activities have been reported to be similar. In addition, prior studies have shown that pegylation does not detectably alter the secondary or tertiary conformation of the IFN- α 2 core protein as well as for both the 12 kD PEG-IFN- α 2b and 40 kD PEG-IFN- α 2a (9). Thus, the site of pegylation and size of PEG moiety would appear to be the critical elements influencing the relative activities of 12 kD PEG-IFN- α 2b and 40 kD PEG-IFN- α 2a.

The size of the PEG moiety increased the aM_r of the pegylated molecule in excess of the additive empirical molecular weight of the PEG to IFN- α 2 core protein. This is due, in part, to the effect of the hydrophilic nature of PEG polymers on the Stokes radius of the pegylated molecule. Increases in linear PEG molecules from 5 kD to 20 kD resulted in increased aM_r from 23.1 kD for un-pegylated IFN- α 2b to 320.6 kD for 20 kD PEG-IFN- α 2b. Modification in PEG structures also impacted aM_r . Branching two 10 kD PEG

molecules to make 20 kD PEG decreased the M_r from 320.6 kD to 272.3 kD, whereas, conjugating two 20 kD PEG molecules as separate di-pegylated moieties onto a single IFN- α 2b core protein increased the M_r to 639.7 kD. Thus, increasing PEG moiety size could potentially impact the IFN- α 2 core protein when the PEG IFN- α 2 is presented to the interferon alpha receptor.

The relative difference in STAT1 translocation activity that we observed between the 12 kD PEG-IFN- α 2b and the 40 kD PEG-IFN- α 2a was approximately 30 to 1 and consistent with their relative anti-viral and anti-proliferative activities. Several laboratories have reported that IFN- α 2 anti-viral and anti-proliferative activity *in vitro* is dependent upon JAK/STAT signaling through a potentially rate-limited interaction with the IFNAR1/IFNAR2 heterodimeric receptor complex (21-23). IFN- α 2 binds to the IFNAR1/IFNAR2 heterodimeric complex activating the JAK1 and Tyk2 kinases. This leads to phosphorylation and dimerization of STAT1 and STAT2 and subsequent translocation of the dimer to the nucleus with IRF-9 (24-27). Translocation is required for the dimer to form the ISGF-3 complex and bind to the ISRE element that in turn initiates the transcription of IFN- α inducible genes (28). The advantage of using a STAT1 translocation assay for signaling assessment is that the translocation event is linked to both the receptor-ligand interaction and the ultimate expression of IFN- α gene transcription, which is necessary for anti-viral and anti-proliferative activity.

It seems likely that the very different distributions of positional isomers for 12 kD PEG-IFN- α 2b and 40 kD PEG-IFN- α 2a may contribute substantially to their differences in *in*

vitro activity. The His³⁴ positional isomer is the major isomer in 12 kD PEG-IFN- α 2b due to the chemical conditions used for the SC-PEG conjugation (29). The remaining positional isomers for 12 kD PEG-IFN- α 2b are predominantly lysine conjugates (9). In contrast, 40 kD PEG-IFN- α 2a comprises almost completely lysine positional isomers and includes no histidine positional isomers (11). The 12 kD PEG-IFN- α 2b and 40 kD PEG-IFN- α 2a share positional isomers at Lys³¹, Lys⁸³, Lys¹²¹, Lys¹³¹, and Lys¹³⁴, though in different distributions. Significantly, the His³⁴ positional isomer demonstrated a consistently lower ED₅₀ for induction of STAT1 translocation than any of the other positional isomers studied. Conversely, the Lys³¹ positional isomer had one of the highest ED₅₀s for induction of STAT1 translocation. The difference in activity for these 2 positional isomers may seem surprising since they are located in close proximity on the AB1 loop (amino acids 22-51) of IFN- α 2, which appears to be involved in 1 of 2 putative binding domains for IFNAR2 (30-33).

There are several potential explanations for difference in activity of the His³⁴ and Lys³¹ positional isomers. One potential explanation for the higher activity of His³⁴ is depegylation either prior to, or associated with, binding to IFNAR2. This would result in free IFN- α 2 that could have more favorable reaction kinetics with the receptor. Two results argue against this possibility. Measurements of pegylated and free His³⁴ IFN- α 2, in culture medium under conditions used for the STAT1 translocation assay, revealed that free IFN- α 2 levels were too low to account for the significantly higher activity of the His³⁴ isomer and that no significant free IFN- α 2 formed during the experiment. Second, the attenuation of His³⁴ positional isomer anti-viral activity with 20 kD and 30 kD PEGs

would not have been observed if the signal had been transmitted by depegylated, free IFN- α 2b. The more likely reason for higher activity with the His³⁴ isomer is that the site of pegylation may reduce the impact of steric hindrance from the PEG molecule.

Roisman et al described the free energy of association interaction between IFN- α 2 and IFNAR2 through 2 domains: the deep insertion of the 45-52 loop of IFNAR2 into a groove in IFN- α 2 formed around Ala¹⁴⁵ on the E-helix (amino acids 137-156) and an interaction with the central part of the IFN- α 2 E-helix at Arg¹⁴⁹ and Ser¹⁵² with the 76-82 loop of IFNAR2 (31). Arg³³ may make 2 potential hydrogen bonds on the AB1 loop of IFN- α 2 through its side chain with the backbone oxygens of Ser⁴⁹ and Lys⁵⁰ on the 45-52 IFNAR2 loop. Additional interactions at Phe²⁷ and Asp³⁵ in the AB1 loop of IFN- α 2 may also exist with the 45-52 IFNAR2 loop (31,34). However, the striking discrepancy in activity between 2 closely related positional isomers on the AB1 loop, His³⁴ and Lys³¹, suggests that tertiary positioning of the pegylation site may be involved in disrupting interaction with the receptor. A recent model of IFN- α 2b dimer binding to IFNAR1/IFNAR2 based on X-ray crystallography suggests that His³⁴ is not located at the receptor interface, but rather at the IFN- α 2b dimer interface (34). While pegylation at the His³⁴ site may appear favorable for retaining the activity of IFN- α 2b, the addition of larger PEG molecules (i.e., >12 kD) can quickly limit anti-viral activity for this isomer. This suggests that there is an upper limit of PEG size at His³⁴ between 12 kD and 20 kD, or between a Stoke's radius of 46.4 Å and 56.5 Å. The binding surface area between IFN- α 2 and IFNAR2 resides at 2 domains and has been calculated to be about 2450 Å² (31). Since the surface area for 5 kD His³⁴ PEG-IFN- α 2b is around 3545 Å², much of the PEG molecule would have to be directed away from interacting into the binding domains.

However, as the surface area for 12 kD and 20 kD His³⁴ PEG-IFN- α 2b increases to 6760 A² and 10,023 A², respectively, the PEG molecule may begin to significantly encroach into the binding domain. Alternatively, increased steric hindrance at the dimer binding interface may also contribute to the decreased activity observed with increased PEG molecule size, either cooperatively with, or independently of, the receptor binding interaction.

The Lys¹²¹, Lys¹³¹, and Lys¹³⁴ positional isomers reside on the D-helix of IFN- α 2b. The low STAT1 translocation and anti-viral activity observed with the Lys¹²¹ and Lys¹³¹ positional isomers suggests that pegylation at these sites is also unfavorable. These 2 sites are close to both the AB1 loop area and E-helix groove of IFN- α 2b. Interestingly, the Lys¹³⁴ positional isomer had higher STAT1 translocation and anti-viral activity. This site is located in the DE loop of IFN- α 2b, suggesting that steric hindrance from a PEG molecule at the Lys¹³⁴ site is less than at either Lys¹²¹ or Lys¹³¹. Lys⁸³ is reported to be located at an interaction point between IFN- α 2b and IFNAR1, so it is reasonable to observe diminished activity with this positional isomer (34). Finally, the Cys¹ site was found to be particularly sensitive to pegylation. The structural relevance of this site is important as it is absolutely conserved; in the NH₂-terminus portion of IFN- α this has been shown to be important in mediating anti-viral activity (33, 35).

Another possible explanation for diminished activity based on the site of pegylation is differential influence on IFN- α 2b and IFNAR1/IFNAR2 interaction kinetics (21,36). For example, it has been postulated that the charge loss associated with His³⁴ pegylation may

perturb the electrostatic potential at or near the receptor binding site less than with ϵ -amine pegylation (15). However, it should be noted that Piehler and Schreiber have observed that the IFN- α binding site on IFNAR2 is not a highly negatively charged area on the protein surface, and this limits the potential role for electrostatic forces in determining the rate of association (37). Nevertheless, a cooperative interaction, first through electrostatic steering, followed by docking of the IFN- α 2b and IFNAR2 and IFNAR1, might be impacted by the pegylation.

It is also possible that the site of pegylation in conjunction with size-mediated steric hindrance might cause the core IFN- α protein to be presented in a different contextual interaction with the heterodimeric receptor such that unique recognition domains are not engaged. There have been many reports of differential activity conferred by different IFN- α species with the intact receptor (35). Hybrid IFN- α recombinants have been shown to have specific domains for anti-viral activity (35, 38), anti-proliferative activity (39), and cytotoxic activity (40-42). Studies using human IFN- α 2a/2c hybrids have shown that the N-terminus region and the hydrophobic residues on the C-helix region are particularly important for anti-proliferative activity (43). Splice variants of the human IFNAR1 have been shown to differentially recognize different IFN- α 's through unique receptor subdomains for MHC Class I antigen expression (44). PEG-IFN- α 2b has been shown to have roughly equivalent reductions in the anti-viral, anti-proliferative, cytotoxic, and MHC Class I expression activities, suggesting that the sites of pegylation and the 12 kD size PEG molecule impact these potential recognition domains on the heterodimeric receptor equivalently (9). In these studies, we confirmed that PEG –IFN-

α 2a lost approximately equivalent activity in the anti-viral and anti-proliferative assays, although significantly more activity was lost than that observed for PEG-IFN- α 2b. This suggests similar domain recognition may exist even with the differences in site-of-pegylation and size of the PEG molecule for PEG-IFN- α 2a and PEG-IFN- α 2b.

In light of our results, it is interesting to note that both anti-viral and anti-proliferative activity *in vitro* is transduced by a relatively small receptor occupancy that appears to be independent of mass action but dependent on continuity of signal induction (22,37) Site of pegylation and PEG molecule size both significantly effect *in vitro* signaling of IFN- α 2b, suggesting that a discontinuity in signaling may be occurring as a result of a decreased K_{on} rate. This may have important clinical implications since K_{on} rate is critical for receptor-mediated signaling. Another clinically important component is the serum residency time of the molecule. Pegylation of IFN- α significantly increases the serum residency and thus the number of potential interactions with the receptor. However, at the same time, pegylation decreases the ability of IFN- α to interact with its receptor once it reaches the cell surface. These two consequences of pegylation are likely to have opposing effects on the clinical utility of the resulting preparations, and they must be carefully balanced in the design of PEG-IFN- α s.

Conclusion

The higher *in vitro* specific activity of 12 kD PEG-IFN- α 2b relative to 40 kD PEG-IFN- α 2a can be attributed to differences in the respective size of the PEG moiety and the distribution of positional isomers. This study provides evidence that the overall *in vitro* activity of PEG-IFN- α s is governed both by PEG moiety size and by specific positional isomers. In particular, the 12 kD PEG-His³⁴ positional isomer, a major constituent of 12 kD PEG-IFN- α 2b, retained the highest post-pegylation specific activity. This activity was significantly higher for *in vitro* anti-viral activity compared with all other isomers studied. The higher activity for 12 kD PEG-IFN- α 2b was observed to occur as early as the STAT1 translocation step within the IFN α mediated JAK/STAT signaling pathway. However, increasing the PEG moiety size significantly attenuated the *in vitro* anti-viral activity of all pegylation sites studied. The correlative effects of site and size of pegylation observed with the anti-viral, anti-proliferation, and STAT1 translocation activity point to a receptor mediated mechanism. Unfortunately, extant reported clinical studies have not been appropriately balanced by protein-weight to help clearly elucidate the impact of any receptor mediated activity on *in vivo* efficacy. Further study of the *in vitro* effects of pegylation and the subsequent impact on *in vivo* efficacy are needed to improve our understanding of the optimal balance of receptor-mediated activity against extended serum half-life.

Acknowledgments

The authors would like to thank Dr. Nicholas Murgolo (Schering-Plough Research Institute) for his expert review on IFN- α 2b structure and binding to the heterodimeric receptor.

REFERENCES

1. Seeff, L. B., and Hoofnagle, J. H. (2003) *Clin Liver Dis* **7**, 261-287
2. Glue, P., Fang, J. W., Rouzier-Panis, R., Raffanel, C., Sabo, R., Gupta, S. K., Salfi, M., and Jacobs, S. (2000) *Clin Pharmacol Ther* **68**, 556-567
3. (2004) *Prescribing information:PEG-Intron (peginterferon alfa-2b) powder for injection (2004)*. Physicians' Desk Reference, Thomson PDR, Montvale, NJ
4. Luxon, B. A., Grace, M., Brassard, D., and Bordens, R. (2002) *Clin Ther* **24**, 1363-1383
5. Lindsay, K. L., Trepo, C., Heintges, T., Shiffman, M. L., Gordon, S. C., Hoefs, J. C., Schiff, E. R., Goodman, Z. D., Laughlin, M., Yao, R., and Albrecht, J. K. (2001) *Hepatology* **34**, 395-403
6. Zeuzem, S., Feinman, S. V., Rasenack, J., Heathcote, E. J., Lai, M. Y., Gane, E., O'Grady, J., Reichen, J., Diago, M., Lin, A., Hoffman, J., and Brunda, M. J. (2000) *N Engl J Med* **343**, 1666-1672
7. Heathcote, E. J., Shiffman, M. L., Cooksley, W. G., Dusheiko, G. M., Lee, S. S., Balart, L., Reindollar, R., Reddy, R. K., Wright, T. L., Lin, A., Hoffman, J., and De Pamphilis, J. (2000) *N Engl J Med* **343**, 1673-1680
8. van Der Auwera, P., Platzer, E., Xu, Z. X., Schulz, R., Feugeas, O., Capdeville, R., and Edwards, D. J. (2001) *Am J Hematol* **66**, 245-251
9. Grace, M., Youngster, S., Gitlin, G., Sydor, W., Xie, L., Westreich, L., Jacobs, S., Brassard, D., Bausch, J., and Bordens, R. (2001) *J Interferon Cytokine Res* **21**, 1103-1115

10. Bailon, P., Palleroni, A., Schaffer, C. A., Spence, C. L., Fung, W. J., Porter, J. E., Ehrlich, G. K., Pan, W., Xu, Z. X., Modi, M. W., Farid, A., Berthold, W., and Graves, M. (2001) *Bioconjug Chem* **12**, 195-202
11. Foser, S., Schacher, A., Weyer, K. A., Brugger, D., Dietel, E., Marti, S., and Schreitmuller, T. (2003) *Protein Expr Purif* **30**, 78-87
12. Youngster, S., Wang, Y. S., Grace, M., Bausch, J., Bordens, R., and Wyss, D. F. (2002) *Curr Pharm Des* **8**, 2139-2157
13. Felix, A. M., Lu, Y. A., and Campbell, R. M. (1995) *Int J Pept Protein Res* **46**, 253-264
14. Meager, A., Gaines Das, R., Zoon, K., and Mire-Sluis, A. (2001) *J Immunol Methods* **257**, 17-33
15. Wylie, D. C., Voloch, M., Lee, S., Liu, Y. H., Cannon-Carlson, S., Cutler, C., and Pramanik, B. (2001) *Pharm Res* **18**, 1354-1360
16. Ding, G. J., Fischer, P. A., Boltz, R. C., Schmidt, J. A., Colaianne, J. J., Gough, A., Rubin, R. A., and Miller, D. K. (1998) *J Biol Chem* **273**, 28897-28905
17. Forti, R. L., Schuffman, S. S., Davies, H. A., and Mitchell, W. M. (1986) *Methods Enzymol* **119**, 533-540
18. Knauf, M. J., Bell, D. P., Hirtzer, P., Luo, Z. P., Young, J. D., and Katre, N. V. (1988) *J Biol Chem* **263**, 15064-15070
19. Monkarsh, S. P., Ma, Y., Aglione, A., Bailon, P., Ciolek, D., DeBarbieri, B., Graves, M. C., Hollfelder, K., Michel, H., Palleroni, A., Porter, J. E., Russoman, E., Roy, S., and Pan, Y. C. (1997) *Anal Biochem* **247**, 434-440
20. Kozlowski, A., Charles, S. A., and Harris, J. M. (2001) *BioDrugs* **15**, 419-429

21. Piehler, J., Roisman, L. C., and Schreiber, G. (2000) *J Biol Chem* **275**, 40425-40433
22. Lee, C. K., Bluysen, H. A., and Levy, D. E. (1997) *J Biol Chem* **272**, 21872-21877
23. Pestka, S. (1997) *Semin Oncol* **24**, S9-18-S19-40
24. Samuel, C. E. (2001) *Clin Microbiol Rev* **14**, 778-809, table of contents
25. Darnell, J. E., Jr., Kerr, I. M., and Stark, G. R. (1994) *Science* **264**, 1415-1421
26. Leonard, W. J. (1996) *Nat Med* **2**, 968-969
27. Horvath, C. M., and Darnell, J. E. (1997) *Curr Opin Cell Biol* **9**, 233-239
28. Stark, G. R., Kerr, I. M., Williams, B. R., Silverman, R. H., and Schreiber, R. D. (1998) *Annu Rev Biochem* **67**, 227-264
29. Wang, Y. S., Youngster, S., Bausch, J., Zhang, R., McNemar, C., and Wyss, D. F. (2000) *Biochemistry* **39**, 10634-10640
30. Radhakrishnan, R., Walter, L. J., Hruza, A., Reichert, P., Trotta, P. P., Nagabhushan, T. L., and Walter, M. R. (1996) *Structure* **4**, 1453-1463
31. Roisman, L. C., Piehler, J., Trosset, J. Y., Scheraga, H. A., and Schreiber, G. (2001) *Proc Natl Acad Sci U S A* **98**, 13231-13236
32. Walter, M. R. (1997) *Semin Oncol* **24**, S9-52-S59-62
33. Klaus, W., Gsell, B., Labhardt, A. M., Wipf, B., and Senn, H. (1997) *J Mol Biol* **274**, 661-675
34. Nagabhushan, T. L., Reichert, P., Walter, M. R., and Murgolo, N. J. (2002) *Canadian Journal of Chemistry* **80**, 1166-1173

35. Rehberg, E., Kelder, B., Hoal, E. G., and Pestka, S. (1982) *J Biol Chem* **257**, 11497-11502
36. Schreiber, G., and Fersht, A. R. (1996) *Nat Struct Biol* **3**, 427-431
37. Piehler, J., and Schreiber, G. (1999) *J Mol Biol* **289**, 57-67
38. Fish, E. N., Banerjee, K., and Stebbing, N. (1983) *Biochem Biophys Res Commun* **112**, 537-546
39. Hu, R., Gan, Y., Liu, J., Miller, D., and Zoon, K. C. (1993) *J Biol Chem* **268**, 12591-12595
40. Ortaldo, J. R., Mason, A., Rehberg, E., Moschera, J., Kelder, B., Pestka, S., and Herberman, R. B. (1983) *J Biol Chem* **258**, 15011-15015
41. Ortaldo, J. R., Herberman, R. B., Harvey, C., Osheroff, P., Pan, Y. C., Kelder, B., and Pestka, S. (1984) *Proc Natl Acad Sci U S A* **81**, 4926-4929
42. Ortaldo, J. R., Mantovani, A., Hobbs, D., Rubinstein, M., Pestka, S., and Herberman, R. B. (1983) *Int J Cancer* **31**, 285-289
43. Hu, R., Bekisz, J., Schmeisser, H., McPhie, P., and Zoon, K. (2001) *J Immunol* **167**, 1482-1489
44. Cook, J. R., Cleary, C. M., Mariano, T. M., Izotova, L., and Pestka, S. (1996) *J Biol Chem* **271**, 13448-13453

Figure Legends and Table Captions

Table 1

Comparative anti-viral and anti-proliferation activities for 12 kD PEG-IFN- α 2b and 40 kD PEG-IFN- α 2a. 12 kD PEG-IFN- α 2b or 40 kD PEG-IFN- α 2a were diluted in serial 2-fold fashion by IFN- α protein weight. Anti-viral protection was determined using an FS-71/EMCV CPE assay, and anti-proliferative activity was determined using a Daudi cell assay. All titrations were performed in triplicate on plates with a calibrated IFN- α 2b reference standard. The mean titer (IU/ml) was determined at the 50% point of the titration curve and was an average of curves from 3 different experimental days (n=9 curves). Specific activity was calculated using the concentration of the IFN- α 2 protein, independent of weight contribution from PEG. The relative percent of IFN- α 2b activity was calculated using the specific activity of IFN- α 2b at 2.6×10^8 IU/mg.

Table 2

Effect of PEG mdecule size on eM_r of PEG-IFN- α .

Figure 1a & b

a. Separation of His³⁴ and Cys¹ Positional Isomers from Mono-PEG-IFN- α 2b

Produced at a Reaction pH of 6.5 by Preparative Scale Cation-Exchange Chromatography

b. Separation of Lysine Positional Isomers from Mono-PEG-IFN- α 2b Produced at a Reaction pH of 10 by Preparative Scale Cation-Exchange Chromatography

IFN- α 2b was pegylated with SC-PEG 5 kD, SC-PEG 12 kD, SC-PEG 20 kD, and SC-PEG 30 kD linkers at a reaction pH of 6.5 to produce His³⁴ and Cys¹ positional isomers and reaction pH of 10 to produce lysine-modified positional isomers. The mono-pegylated reaction products were isolated by size exclusion chromatography and then resolved into individual positional isomers by HPIEX. The elution profiles of the ion-exchange chromatographies are shown in Figures 1a and 1b.

Figure 2 (A-G)

STAT1 translocation responses of pegylated positional isomers of IFN- α 2b.

Equivalent weight concentrations of IFN- α 2b mono-pegylated 5, 12, 20, 30-kD positional isomers were diluted in serial 3-fold fashion in quadruplicate for stimulation of STAT1 translocation in Huh-7 cells. Control curves using 12 kD PEG-IFN- α 2b and 40 kD PEG-IFN- α 2a were run on each plate. STAT1 translocation data are expressed as the quadruplicate mean \pm SEM normalized for the percent of cell control. The percent of cell control was calculated as the percent of fluorescent intensity of the well relative to the mean fluorescent intensity of the cell control wells.

Figure 3

STAT1 translocation ED₅₀s for pegylated positional isomers of IFN- α 2b. The ED₅₀ for each dose-response curve for STAT1 translocation (n=4) was determined from the 50% inflection point of a 4-parameter curve fit using Softmax Pro v4.3 software. The mean, \pm SEM are summarized for each positional isomer and size of PEG. An ANOVA, using Student's t-test (p<0.05), was carried out comparing positional isomers within each PEG size using JMP v5.0.1 software. In instances of unequal variances among groups, the Welch ANOVA test was used to confirm statistically significant differences. All statistically significant differences (p<0.05) are reported compared with the H34 isomer within each PEG size group: *within 5 kD PEG size; #within 12 kD PEG size; \$within 20 kD PEG size; & within 30 kD PEG size.

Figure 4

Anti-viral protection titers for pegylated positional isomers of IFN- α 2b. Anti-viral protection activity was measured using FS-71 cells infected with EMCV. The anti-viral titer was calculated by direct comparison of the 50% endpoint for each sample to the 50% endpoint for the IFN standard using a 4-parameter fit generated by ALLWIN v2.03 software. The mean anti-viral titer \pm SEM are summarized for each positional isomer and size of PEG. An ANOVA using Student's t-test (p<0.05) was carried out comparing positional isomers within each PEG size using JMP v5.0.1 software. All statistically significant differences (p<0.05) are reported compared with the His³⁴ isomer within each PEG size group: *within 5 kD PEG size; #within 12 kD PEG size; \$within 20 kD PEG size; & within 30 kD PEG size.

Table 1

	Mean Titer	Std. Dev.	Specific Activity	Percent of IFN-α2b
	(IU/ml)	(IU/ml)	(IU/mg)	Activity
<i>FS-71 anti-viral protection assay</i>				
12 kD PEG-IFN- α 2b	1.65×10^7	5.05×10^6	6.61×10^7	25.4
40 kD PEG-IFN- α 2a	5.90×10^5	1.24×10^5	3.15×10^6	1.2
<i>A549 anti-viral protection assay</i>				
12 kD PEG-IFN- α 2b	1.37×10^7	1.44×10^6	9.00×10^7	34.6
40 kD PEG-IFN- α 2a	5.85×10^5	1.08×10^5	3.13×10^6	1.2
<i>Daudi anti-proliferation assay</i>				
12 kD PEG-IFN- α 2b	1.13×10^7	1.35×10^6	7.52×10^7	28.9
40 kD PEG-IFN- α 2a	3.34×10^5	6.01×10^4	1.78×10^6	0.7

Table 2

	MW (kD)	Apparent M_r, (kD)	Calculated Stokes Radius (Å)
IFN- α 2b	23.1	23.1	21.2
5 kD PEG-IFN- α 2b	28.1	73.3	33.6
12 kD PEG-IFN- α 2b (PEG Intron)	35.1	165.6	46.4
branched 20 kD PEG-IFN- α 2b	43.1	272.3	56.5
linear 20 kD PEG-IFN- α 2b	43.1	320.6	60.3
di 20 kD PEG-IFN- α 2b	63.1	639.7	79.4

Figure 1A

A

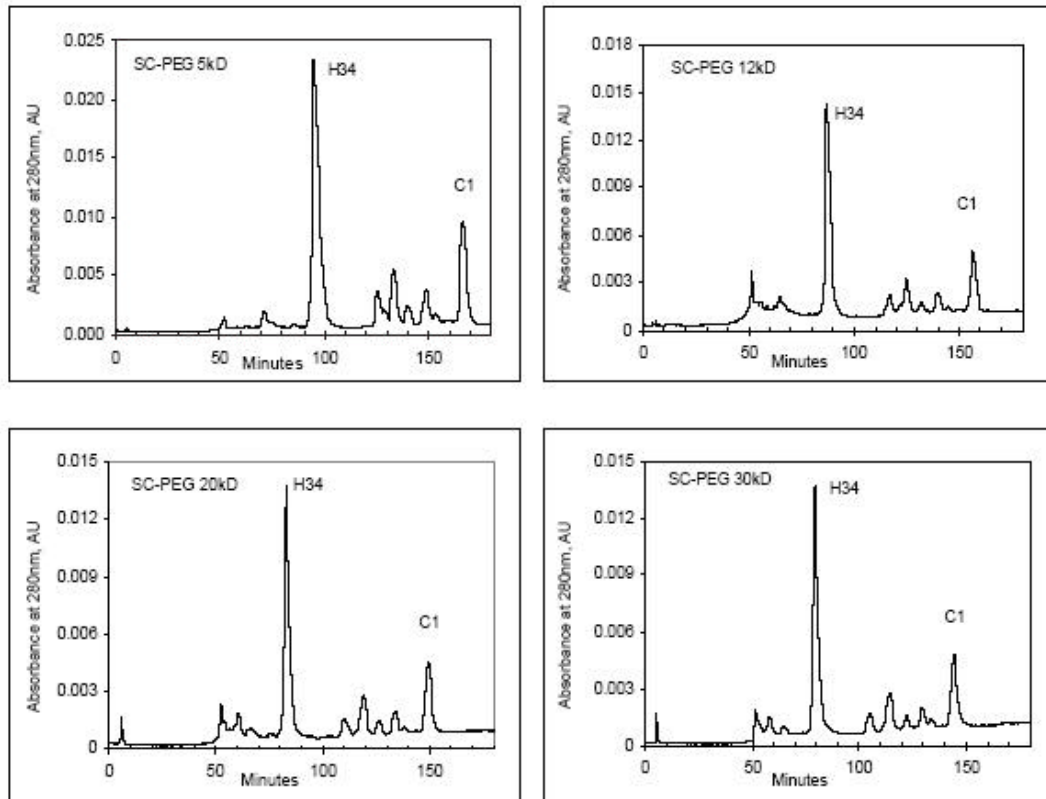


Figure 1B

B

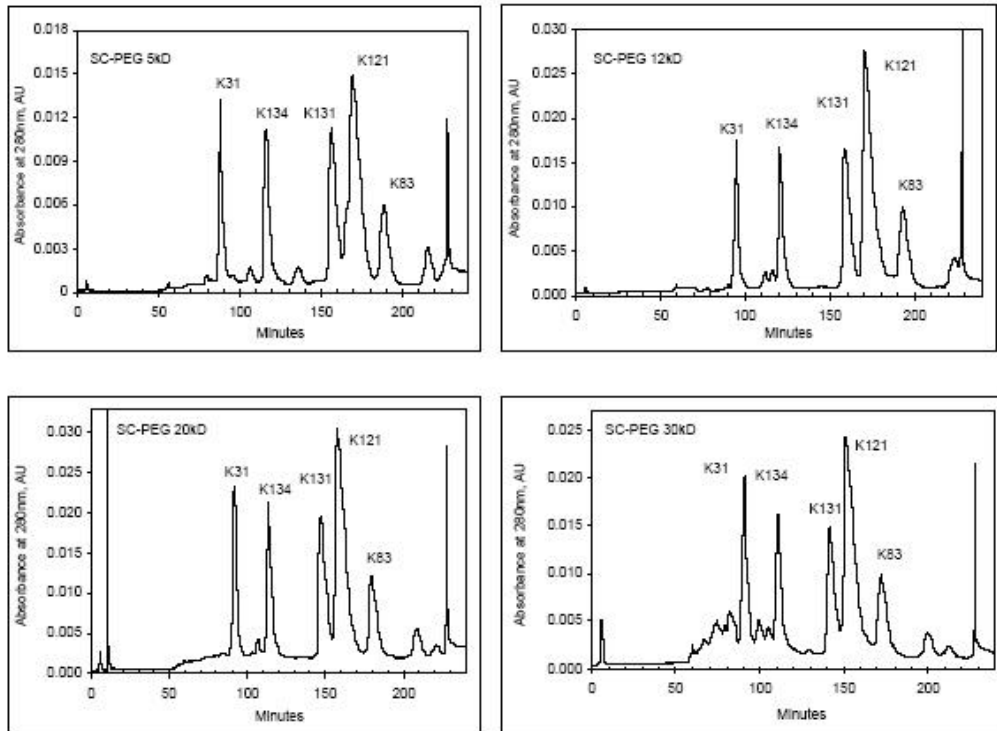


Figure 2A

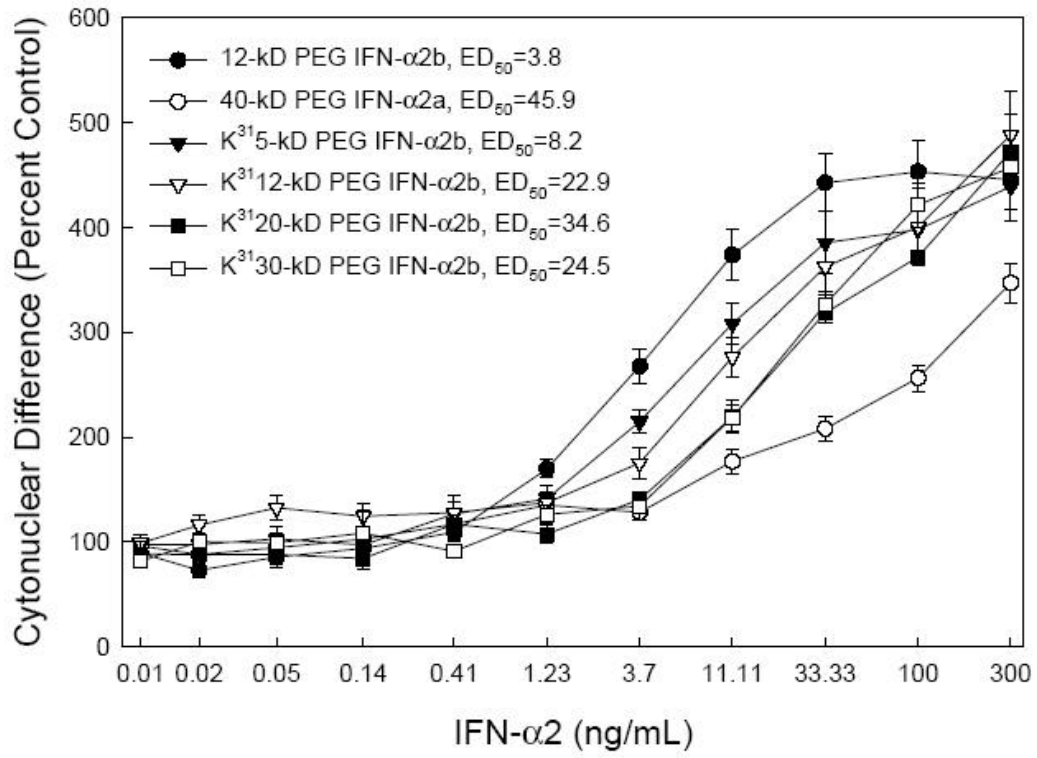


Figure 2B

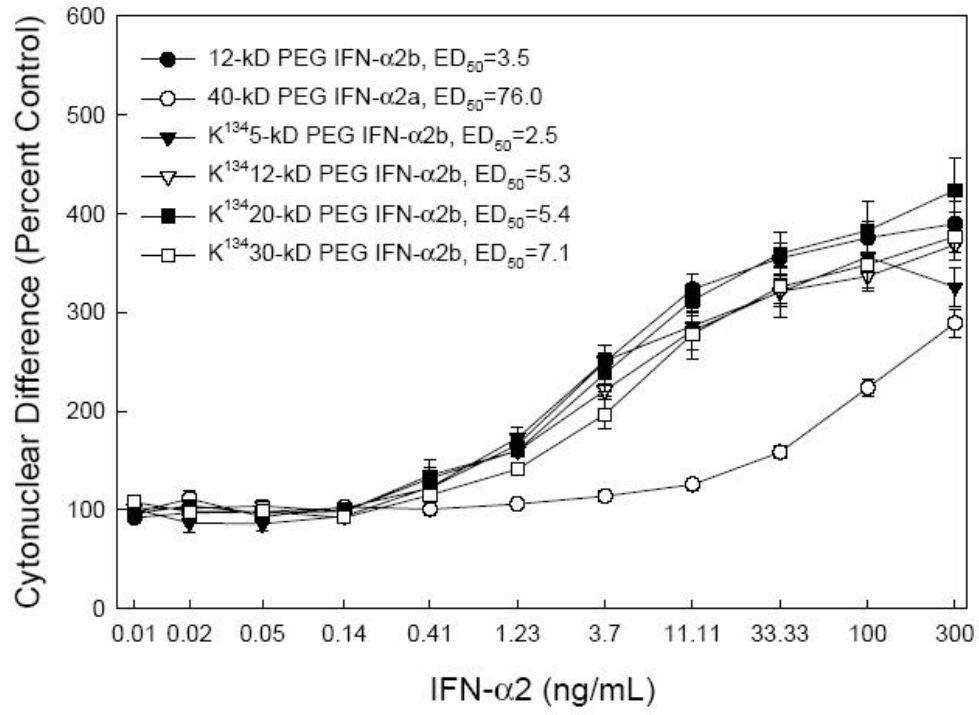


Figure 2C

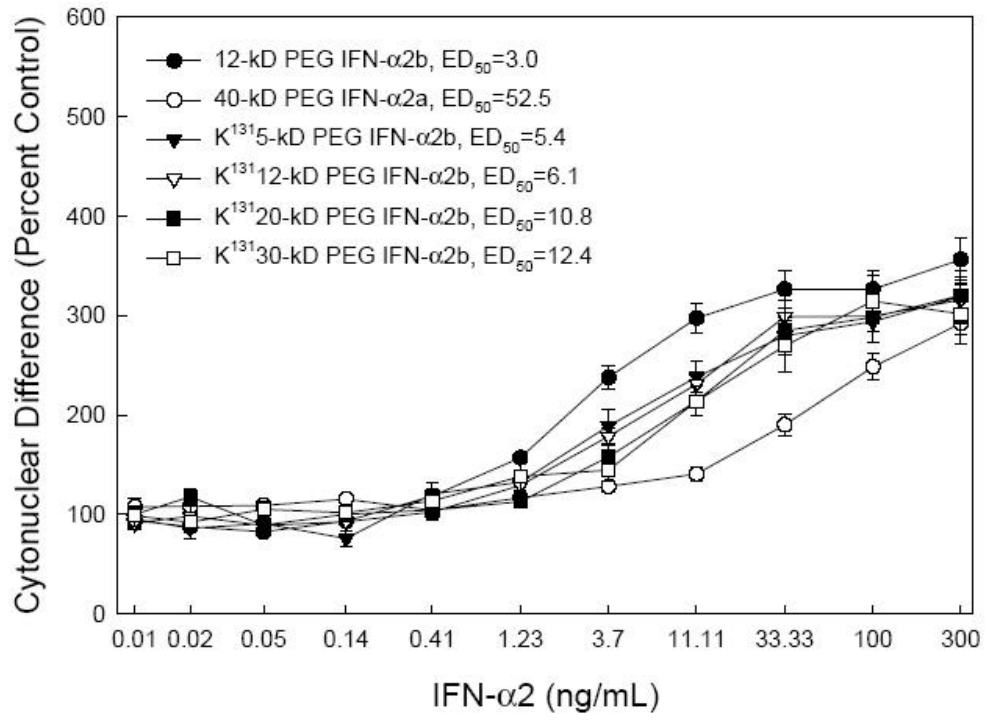


Figure 2D

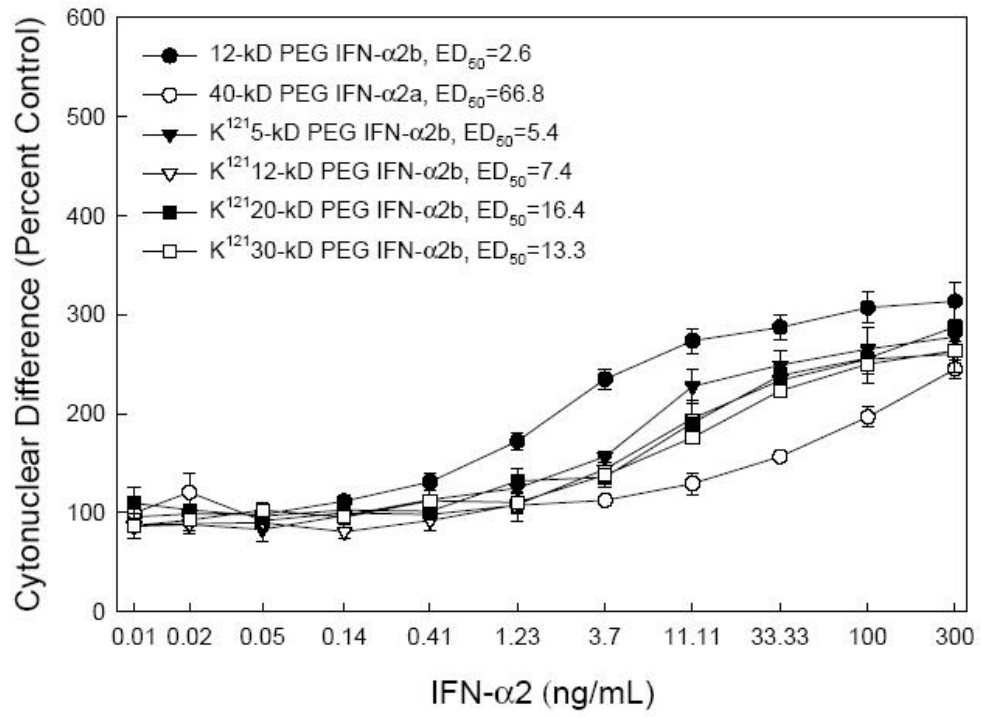


Figure 2E

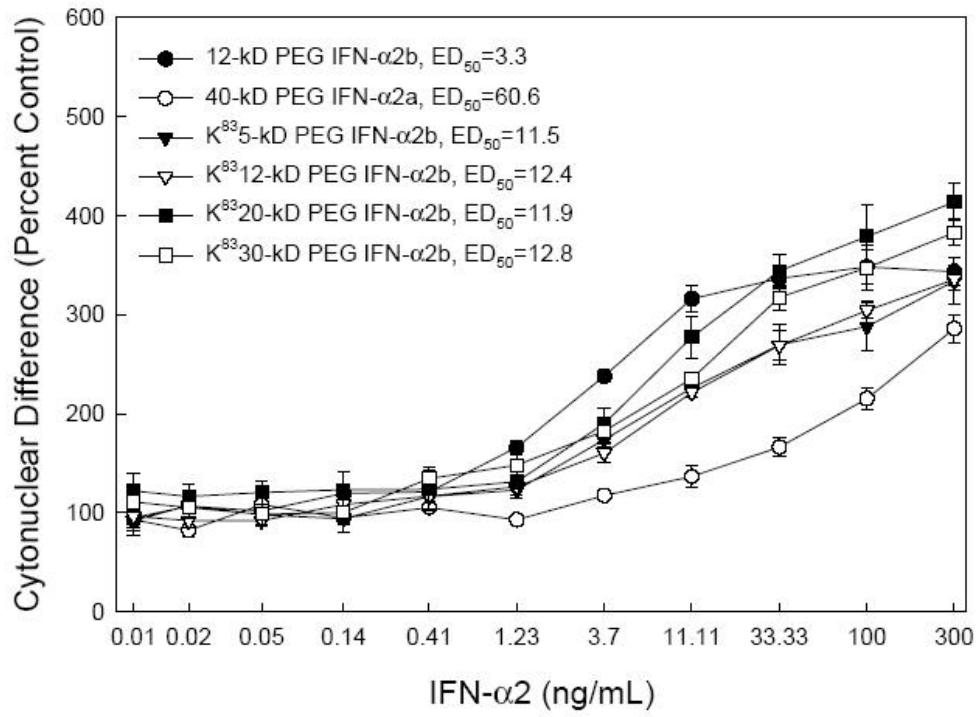


Figure 2F

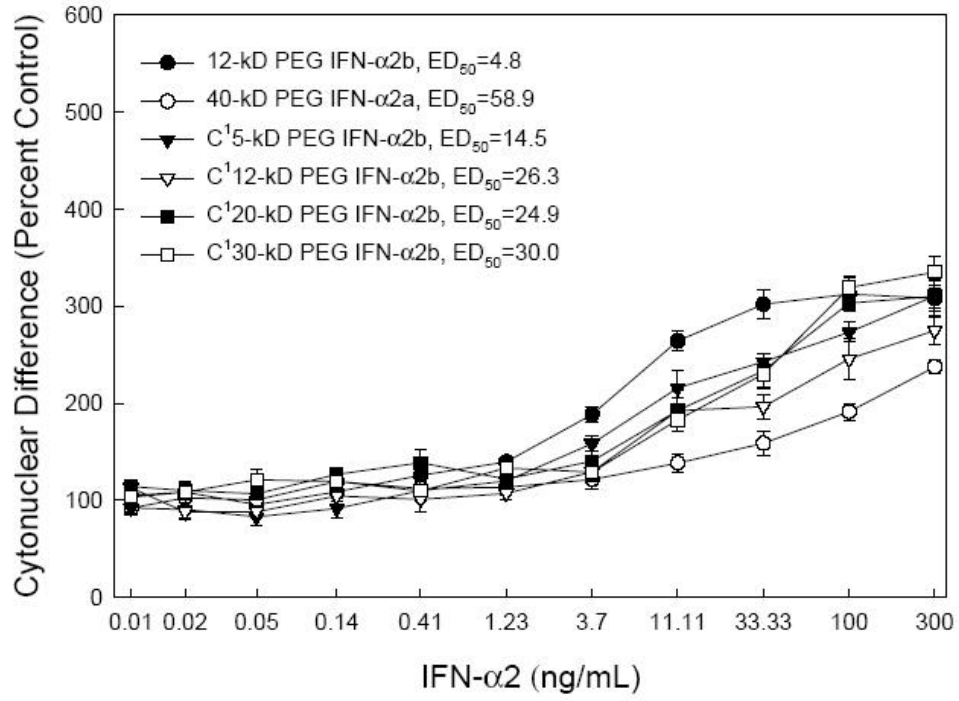


Figure 2G

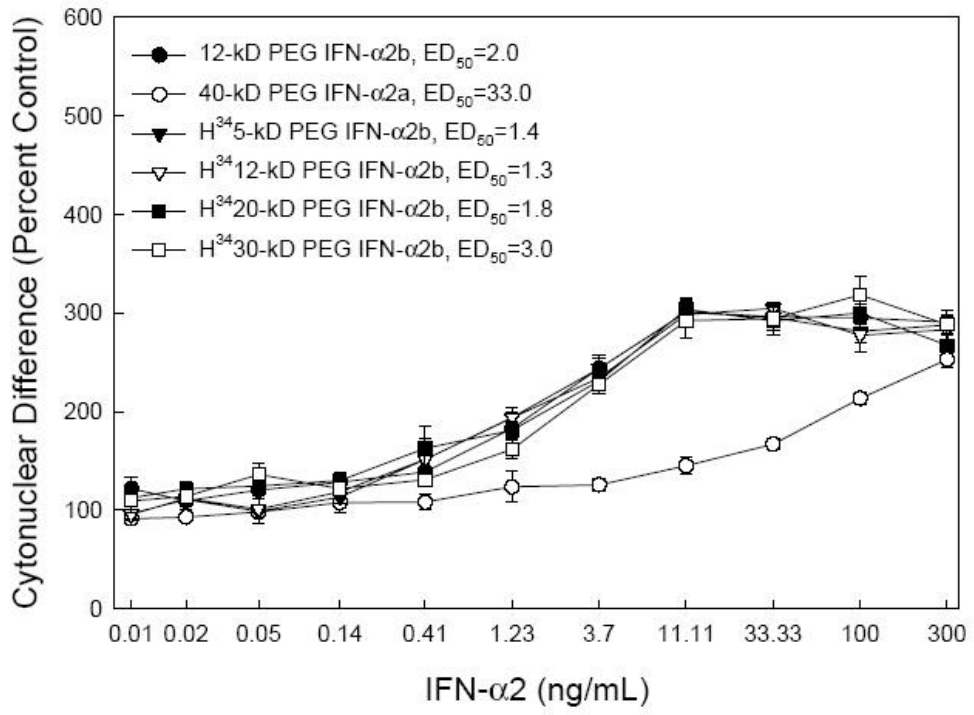


Figure 3

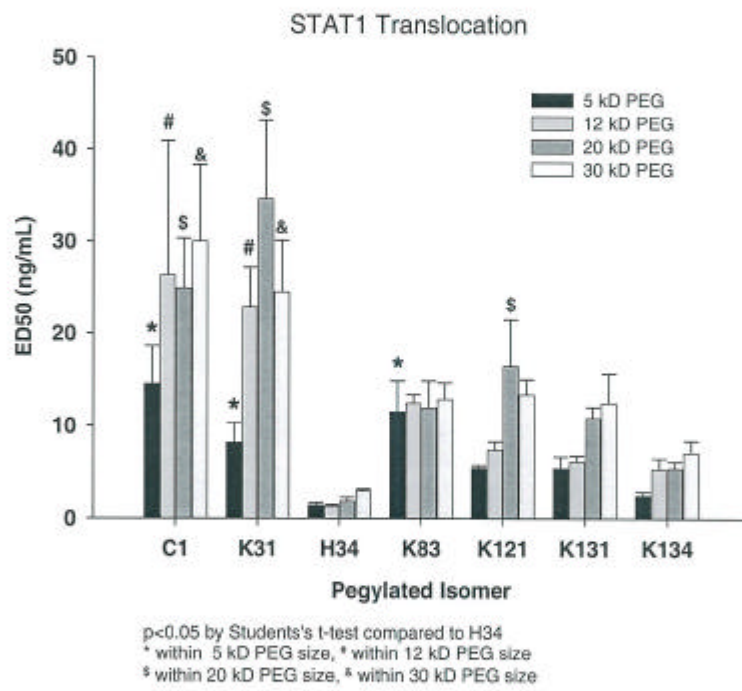


Figure 4

